Chapter

Improved Narrow Water Extraction Using a Morphological Linear Enhancement Technique

Wu Bo, Zhang Jinmu and Zhao Yindi

Abstract

An improved water extraction method using a morphological linear enhancement technique is proposed to improve the delineation of narrow water features for the modified normalized difference water index (MNDWI) derived from remote sensing images. This method introduces a morphological white top-hat (WTH) transforming operation on the MNDWI to extract multi-scale and multidirectional differential morphological profiles and constructs a morphological narrow water index (MNWI). The MNWI can effectively enhance the local contrast of linear objects, allowing narrow water bodies to be easily separated from mountain shadows and other features. Furthermore, to accurately delineate surface water bodies, a dual-threshold segmentation method was also developed by combining an empirical threshold segmentation with the MNDWI for wide water bodies and an automatic threshold segmentation with the MNWI for narrow water bodies. This method was validated using three experimental datasets, which were taken from two different Landsat images. Our results demonstrate that narrow water bodies can be sufficiently identified, with an overall accuracy of over 90%. Most narrow streams or rivers keep a continuous shape in space, and the boundaries of the water bodies are accurately delineated as compared with the MNDWI method. Finally, the proposed method was used to extract the entire inland surface water of Fujian province, China.

Keywords: narrow water extraction, white top-hat transform, MNWI, dual-threshold segmentation

1. Introduction

Surface water is one the most vital earth resources undergoing changes in time and space as a consequence of land use/cover (LULC) changes, climate change, and other forms of environmental changes in many parts of the world. Timely and accurate monitoring and delivery of data of the dynamics of surface water are, therefore, critically important in various scientific disciplines, such as the assessment of present and future water resources, climate models, agricultural suitability, river dynamics, wetland inventory, watershed analysis, surface water surveys, and environmental monitoring [1].

Remote sensing at different spatial, spectral, and temporal resolutions provides an enormous amount of data for mapping water resources and its dynamics at local to global scales. At a result, it has become a routine approach for the monitoring of land surface water bodies, since the acquired data can provide macroscopic, real-time, dynamic, and cost-effective information, which is substantially different from conventional in situ measurements. Various approaches for water body extraction from multispectral images have been developed in the past decades [2–4], which can be broadly grouped into three categories: spectral band segmentation, image supervised classification, and water indices. Among all these methods, of particular interest is the spectral water index-based method, as it is a reliable and cost-effective method. This type of method takes advantage of reflectivity differences of each involved band for water body extraction based on the analysis of signature differences between water and other surfaces.

One of the most widely used indexes is the normalized difference water index (NDWI) [4], which utilizes the green (band 2) and near-infrared (band 4) of Landsat TM to delineate open water features. However, Xu found that the NDWI cannot efficiently suppress the signal from built-up surfaces and therefore proposed an improved one, called modified normalized difference water index (MNDWI) [5], where the NDWI was modified by replacing band 4 with band 5 of Landsat TM/ETM. The MNDWI has been validated as one of the most widely used water indices for various applications, though it is still difficult to obtain a high accuracy of water extraction in complex circumstances. Carleer and Wolff [6], among others, have found that the land cover classifications of water and shadow can often be confused. This issue often arises in environments where a large amount of shadow and water regions exist, such as urban and mountainous landscapes. The identification of narrow water bodies (such as narrow streams, canals, ponds, small reservoirs, etc.) can be a difficult task when using NDWI or MNDWI images, because the shallow and narrow water pixels may generate unstable spectral profiles or characteristics, due to the mixed reflectance caused by sediment and/or adjacent land covers. Narrow water is typically defined as a water body with an apparent width less than or equal to three pixels in an image. Therefore, narrow water features often contain mixed pixels, and the extraction of them from NDWI or MNDWI images generally exhibits a discontinuous shape in space.

To remedy this problem, past studies have attempted to identify narrow water features by combining different procedures. Yang et al. proposed a method of extracting initial water information via a user-defined specified water index, and then they performed a series of operations. These operations include morphological dilation, image filtering, and thinning techniques applied to the water index image to recover the continuity of narrow rivers or streams [7]. This method can be effective in the extraction of narrow water bodies if the water disruption is short; however, it may increase false water identification when water disruption is large, since it is dependent on the morphological dilation operation to reconnect the narrow rivers. Such simple threshold techniques are not often a sufficient solution to identify narrow water bodies; therefore, Li et al. suggested an object-oriented method of small water body extraction [8]. They first extracted textural and shape-related features from images as supplementary information to spectral bands and then performed a segmentation operation on the images using an optimal scale to identify the potential water bodies. Yet, their method is not an automatic process, since it involves multiple user-defined parameters in image segmentation, which prohibits its use in large areas. An alternative approach was performed by Jiang et al. who extracted narrow water features via the enhancement of linear features in NDWI images [9]. However, their procedure involves multiple empirical thresholds, so it is not a cost-effective method for water feature extraction on large scale.

Attempting to improve on these previous approaches, here we propose an automatic water extraction method that constructs a novel narrow water index, denoted as morphological narrow water index (MNWI). The MNWI is constructed using multi-scale and multidirectional differential morphological profiles (DMPs) on a MNDWI image, and then water bodies are automatically extracted using a dual-threshold segmentation. The successful use of DMPs to extract various thematic information from images has been sufficiently validated, such as buildings in urban areas [10, 11], rare earth mining areas [12], and mapping of mangrove forests [13]. In this paper, we introduce a DMP technique to highlight the contrast of bright features as a way of narrow water recognition in the MNDWI images. This can be accomplished because water pixels have higher value than surrounding pixels in MNDWI images. Our approach is expected to improve the ability of narrow water feature identification by enhancing its spatially implicit characteristics using multi-scale morphological features, e.g., other land cover uses that have similar values in a MNDWI image, such as bare patches and shadows, can be easily identified. Our approach also involves a dual-threshold strategy which is adopted for wide and narrow water body extraction, since a simple threshold is not often an adequate solution [14]. An empirical threshold is used first to obtain possible water areas from a MNDWI image, followed by an automatic threshold which is determined by the maximum interclass variance criterion [15] used for extracting narrow water features from a MNWI image. Finally, a logical operation is performed by combining the two potential water features to identify the true water body boundary.

The remainder of this chapter is organized as follows. In Section 2, we describe the MNWI method of narrow water extraction. Experimental results are shown in Section 3 using multiple experiments on TM images, and we use the MNWI method in a practical application for extracting inland water features in Fujian province, China, in Section 4. Finally, Section 5 presents conclusions.

2. The proposed MNWI method

It is well accepted that open and wide water features can be easily separated from other land cover features by using the NDWI or the MNDWI methods, but extracting narrow water boundaries is generally a more difficult task due to its being confused with built-up areas, roads, hill shadows, etc. Therefore, the goal of our proposed MNWI method is the separation of narrow water and other land cover features by depicting the implicit spectral and structural characteristics of MNDWI. Narrow water usually exhibits strong linear shapes and continuous spatial curves; therefore, we propose a linear enhancement operation on a MNDWI image to form a MNWI image, according to the following steps:

Step 1: Generation of a MNWDI image. Level 1 T Landsat images in the study region are first collected, which are then corrected geometrically. Atmospheric and radiometric corrections were then applied using the 6S approach to transform the images into reflectance datasets. Because MNWDI performs better in the extraction of water features than NDWI [5], it is selected for initial water extraction and calculated as:

$$MNDWI = \frac{(Green - MIR)}{(Green + MIR)} \tag{1}$$

where Green and MIR are the image reflectance of the green band and medium-wave infrared band (which correspond to the TM/ETM+ band 5), respectively.

Step 2: Formulation of the MNWI. MNDWI can improve the local contrast between water and other land cover features, since most water bodies can easily be extracted using a threshold segmentation method. However, narrow water bodies are still difficult to extract, as they are easily confused with urban areas, roads, and mountain shadows because of mixed pixels. To alleviate this problem, we adobe a linear object enhancement technique using a white top-hat transform operation on a MNDWI image via the extraction of multi-scale and multidirectional differential morphological profiles to form a MNWI image, according to the following three sub-procedures:

1. **Define linear structures**. A narrow river or stream has clear linear features with two main directions, but the shapes of buildings and mountain shadows have polygon-like features. Hence, we introduce a DMP method to separate them. The use of DMPs involves the designing of a filtering operator (e.g., size and shape), known as a structural element (SE). This acts as a probe to extract or suppress specific structures by checking that each part of the SE fits within the objects in the image. A single-SE size approach is typically not suitable for complex structures; therefore, a series of linear structural elements are implemented to form DMPs, so that the size and directional bias of the narrow water features are identified clearly. Thus, the linear structure element was defined as se = strelem(d, s), where d represents the orientation of the linear structure (e.g., 0°, 45°, 90°, 135°) and s denotes the scale of the small water body.

2. **White-hat morphological reconstruction (white top-hat)**. In general, an opening/closing operator can isolate bright or dark structures in an image when the objects are brighter or darker than the surrounding features. An opening operator can help separate water objects from other land cover features since water appears brighter in a MNDWI image. To isolate features that have a thinner support than a given SE, a common practice to use is a top-hat morphological transform in taking the residual of the opening, closing, and original images to ensure a better shape preservation [11–13]. The white top-hat reconstruction operation is formulated by subtracting the opening operation from the initial image using the same image. This enhances linear features with a structure smaller than the SE, and a morphological reconstruction of the white-hat MNDWI image is according to:

$$WTH(d,s) = MNDWI - \gamma_{MNDWI}(se) \tag{2}$$

where $\gamma_{MNDWI}(se)$ is the output image yielded by performing a closing operator to a MNDWI image. A closing operator can suppress smaller, darker objects and join adjacent objects together; thus we expect that small water bodies smaller than the structural elements will be highlighted after this reconstruction, and open water bodies and background objects larger than the structural elements should be suppressed. We previously defined a narrow water body as no larger than three pixels; thus, the linear structural elements in our algorithm are extended in four directions (0°, 45°, 90°, and 135°), and each direction was applied with three scales ($s_{min} = 1$, $s_{max} = 3$, $\Delta_s = 1$) to generate the WTH image.

3. **Construction of the morphological narrow water index**. The WTH process essentially suppresses the nonrelevant background, though there still may be small features (e.g., buildings or shadows) that must be removed. Narrow water features have linear features with two main orientations, and the difference between maximum and minimum values of the WTH value in different directions is relatively large. Conversely, the shapes of buildings and mountain shadows usually have polygon-like features, indicating that the

WTH difference is small. With this consideration in mind, we determine the contrast of the maximum and minimum values of the WTH in all directions to enhance the linear structure further. Thus, the MNWI is formulated as:

$$MNWI = WTH_{\text{Max}} - WTH_{\text{Min}} \tag{3}$$

where WTH_{Max} and WTH_{Min} are the maximum and the minimum values of the reconstruction of the white top-hat procedure in all directions, respectively.

Step 3: **Dual-threshold segmentation**. A simple threshold is not usually adequate to separate water features in large and complex regions from a MNDWI or MNWI image. Therefore, we employ a dual-threshold strategy to delineate water feature characteristics. A relatively large threshold was first determined empirically to separate the MNDWI image into possible water regions, denoted as W_1. Experimental results suggest that this threshold should be set at 0.2, such that all wide water bodies were extracted, and most other objects were excluded. However, many narrow water bodies may be missed in this procedure, and small rivers may be of a discontinuous shape in space. Thus, another threshold is determined by the Otsu method [15] performed on the MNWI image to extract possible narrow water bodies, denoted as W_2. The final water feature information is then delineated according to the following logical rule: If the possible water in W_2 is connected to any wide water extracted from the MNDWI image (i.e., W_1), it is then determined to be narrow water; otherwise it is categorized as not water.

Step 4: **Image post-processing**. Small trails might also display a high value in a MNWI image and may be misclassified as a narrow water body. To reduce this error, the difference built-up index (NDBI) [16] can also be used to refine the final result. In the present study, a threshold of NDBI >0.05 is used, so that most of the roads and trails are excluded from the final water determinations.

3. Method validations

To evaluate our method, three study regions are taken from two Landsat ETM+/OLI images with different water body types and different terrains, as shown in **Figure 1**. Study area 1 is a sub-scene image with 1000 by 1000 pixel size chosen from a Landsat 7 ETM+ image acquired on September 1, 2001, centered on the Panjiakou Reservoir near Tangshan and Chengde cities in Hebei province in northern China, which covers multiple branches of Luanhe River.

Study area 2 is also a sub-image of 1000 by 1000 pixels, which is located in Luoyuan County, Fujian province, which is acquired from the Landsat 8 operational Landsat image (OLI) on December 13, 2014. This region contains very narrow streams (**Figure 2b**), and it is used to test the extraction ability from mixed pixels. Study area 3 (**Figure 3c**) is a 1000 by 1000 pixel scene selected from the same OLI image as #2, which is located in southern Youxi County, Fujian province, and covers one of main branches of Minjiang River as well as other narrow streams (Qingyin, Qing, Wenjiang, etc.). Youxi County and several villages are in this study area, which contain multiple sources of possible background noise.

Actual water feature information for these study areas are not available, so the water bodies in the three images are manually digitized using high resolution spatial images to provide a basis map for comparison. High-resolution Google Earth™ images were also used as a complementary reference to assist in distinguishing water pixels that might be confused with background noise, such as mountain shadows, trails and built-up areas.

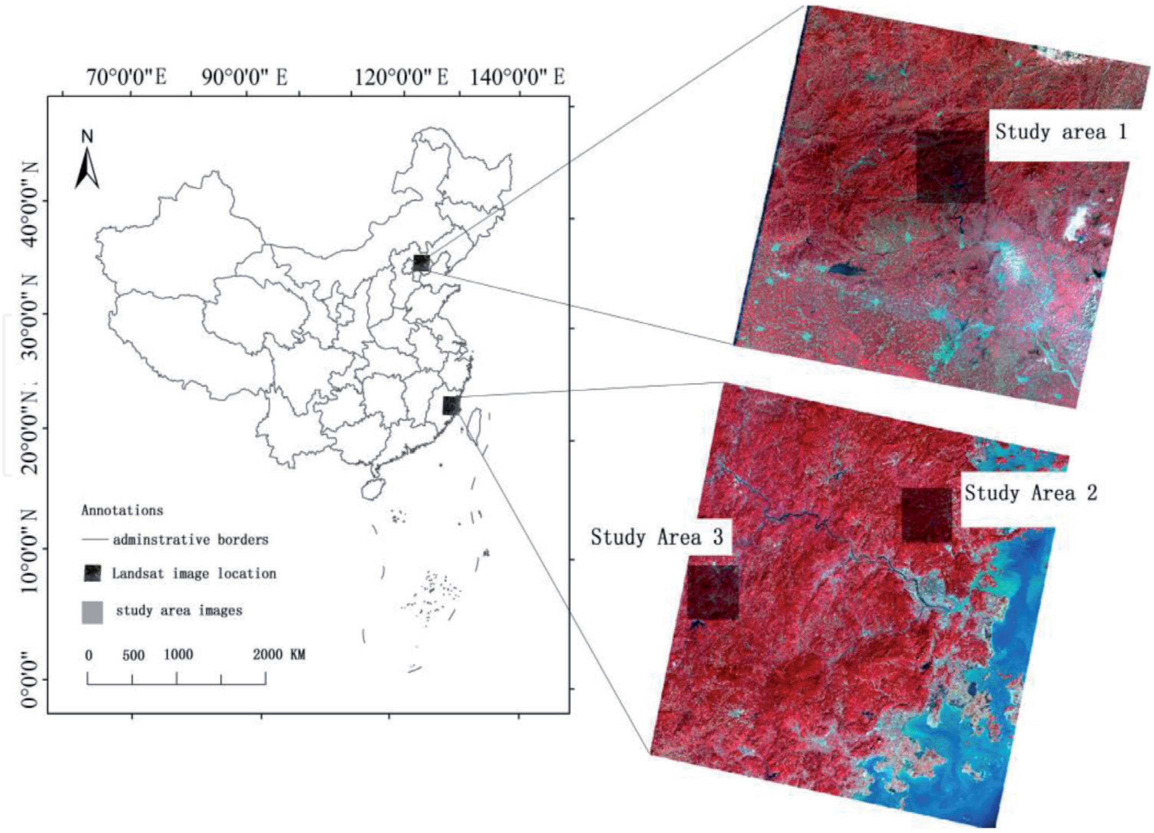

Figure 1.
The collected images and locations for the study areas.

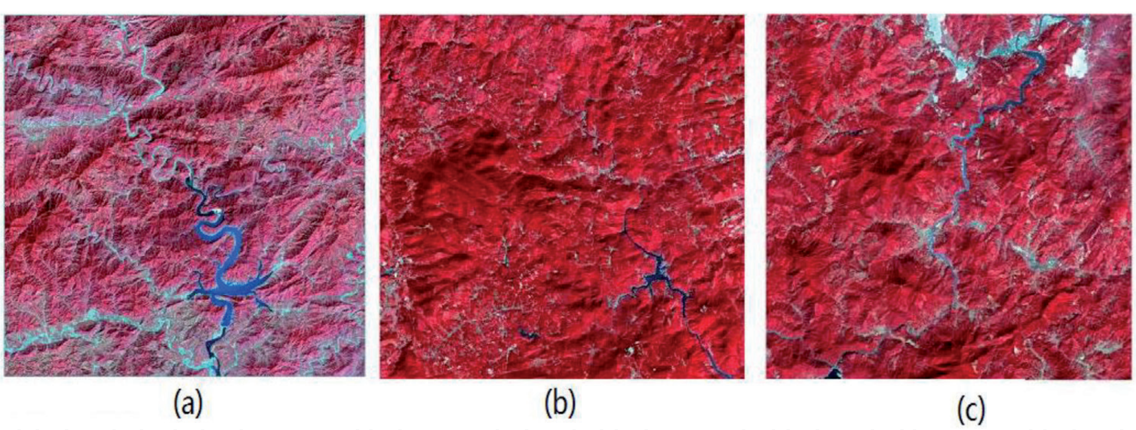

Figure 2.
The false-colored images for the three study areas used in our experiments. (a) study area 1, (b) study area 2, (c) study area 3.

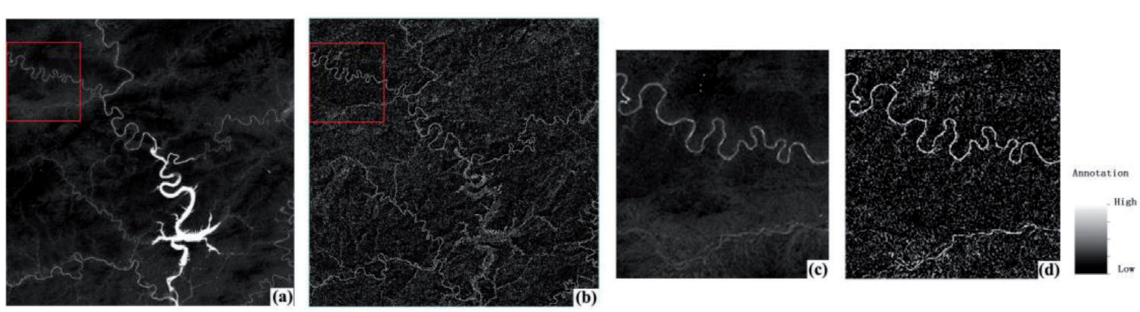

Figure 3.
Comparison of small bodies of water in the MNDWI and the MNWI for study area 1 where (a) and (b) are the extracted water bodies with the MNDWI and the MNWI indexes, respectively, and (c) and (d) denote the focused areas highlighted in red boxes.

3.1 Validation of MNWI features

A comparison between MNDWI and MNWI methods was first described. The two types of water index images for study area 1 are shown in **Figure 3a** and **b**, with focused areas highlighted in red boxes shown in **Figure 3c** and **d**. The pixels' values of water typically have higher values (white areas) than those of the other land cover features in these images, since both the MNDWI and the MNWI water indexes strongly enhance the water body signals. It is also observed in **Figure 3a** and **c** that the brightness difference between wide water and narrow water in the MNDWI image is larger, suggesting that a threshold segmentation on the MNDWI image cannot resolve entire water bodies. In contrast, the difference in the MNWI image is significantly reduced, though they maintain relatively higher values than other land cover features, as shown in **Figure 3b** and **d**. By looking at **Figure 3d**, it is seen that the local contrast between narrow water and other land cover features is significantly enhanced. Additionally, narrow water such as small rivers and branches maintains a continuous spatial shape, suggesting that narrow water features can be accurately extracted with a threshold implementation.

Furthermore, 1200 samples of typical land cover types from study area 3 were randomly selected from each category and were analyzed by calculating the maximal value, the minimal value, the mean value, and the deviation. The criteria for the sample selection are the following: (1) Each land cover has ~200 samples to keep a sample balance; and (2) each land cover contains several small patches from different locations to maintain a spectral variety. **Figure 4** reports the spatial distribution of the samples for study area 3 and their statistical information for six typical land cover types, i.e., wide open water, narrow water, vegetation, built-up area, roads, and shadow. As can be seen in **Figure 4**, the values of the wide water are very high for MNDWI. However, it is difficult to discriminate narrow water from other land cover types, especially for shadows, roads, and built-up areas. In contrast, the values of the narrow water in the MNWI method are relatively high compared with

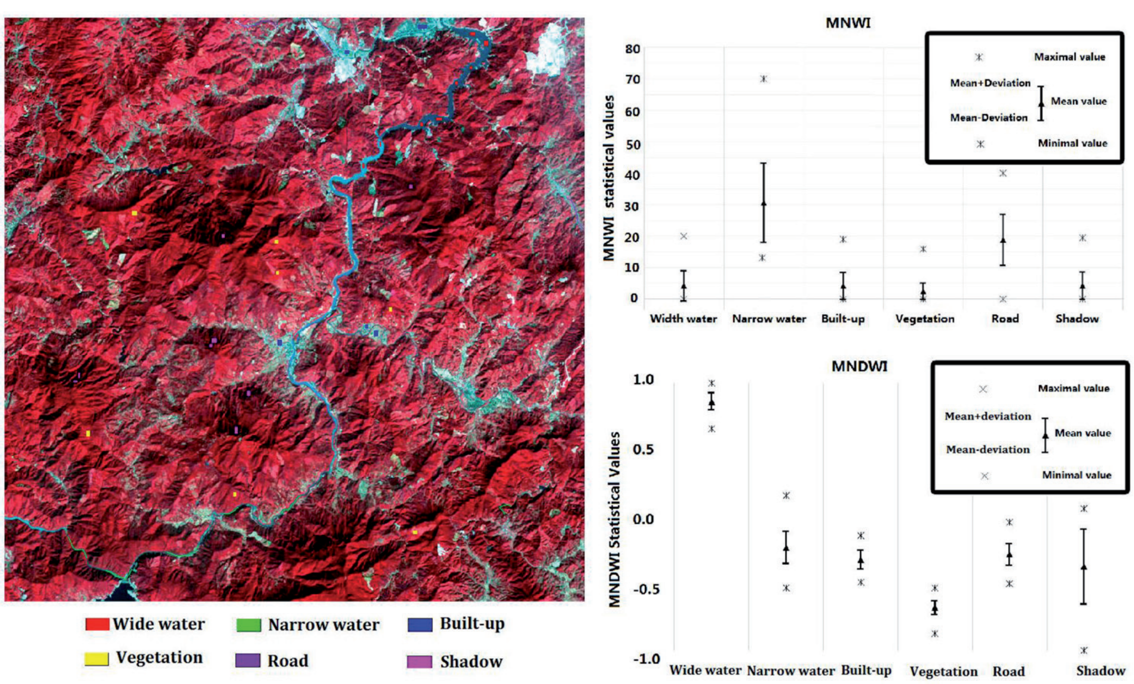

Figure 4.
The spatial distribution of 1200 selected samples for study area 3 (left) and the statistical information of six typical land cover types for MNDWI and MNWI images, respectively (right).

other land cover types, indicating that it is relatively easy to separate the narrow water bodies from other land cover types.

It can also be seen in **Figure 5** that the values of objects with polygon-like shapes, such as wide water, built-up areas, and shadows, are heavily suppressed in the MNWI image since they do not exhibit a linear structure. However, roads also show linear structural characteristics; thus they have high values in a MNWI image. This demonstrates that neither MNDWI nor MNWI can effectively identify entire water bodies using a threshold segmentation. To remedy this, we adopted a dual-threshold strategy. The first threshold is used for wide water extraction from MNDWI, and the second is employed to extract narrow water features from MNWI.

3.2 Validation of dual-threshold segmentation

An empirical threshold (0.2) was first used to perform a rough extraction of potential water features from a MNDWI image; then a second threshold determined by Otsu was determined from the MNWI image for possible narrow water features. Next, a combing procedure was carried out to extract entire water bodies using an "if-then" logic calculation according to the following rule: If two potential water regions are spatially connected, then they are determined to be water bodies; otherwise they are determined to be other land cover types.

As a demonstration of the dual-threshold segmentation method, comparisons between single threshold segmentation of a MNDWI image and dual-threshold segmentation of a MNWI image are shown in **Figure 6(a)–(c)**. It is seen that when a smaller threshold (T = 20) is adopted, a narrow stream keeps a relatively complete spatial shape, yet it also contains a trail (road) at the bottom of the image (**Figure 6a**). However, if we increase the threshold T to 40, this trail is no longer extracted, but the stream exhibits discontinuities along the stream. Thus, the use of a dual-threshold segmentation can better identify this stream as continuous and avoid the identification of the trail.

3.3 Visual assessment

Figure 7 presents the extracted water features using our proposed method for each of the three study areas. As a comparison, water information derived from the MNDWI image using an optimal threshold segmentation is also listed. For clarity, the corrected, misclassified, and omitted water information is labeled with different color schemes. Visual inspection shows that our method significantly outperforms the MNDWI method when using an optimal threshold segmentation. It can be seen that the majority of narrow rivers in each of the study areas are successfully extracted by our method. Six branches of the Luanhe River are

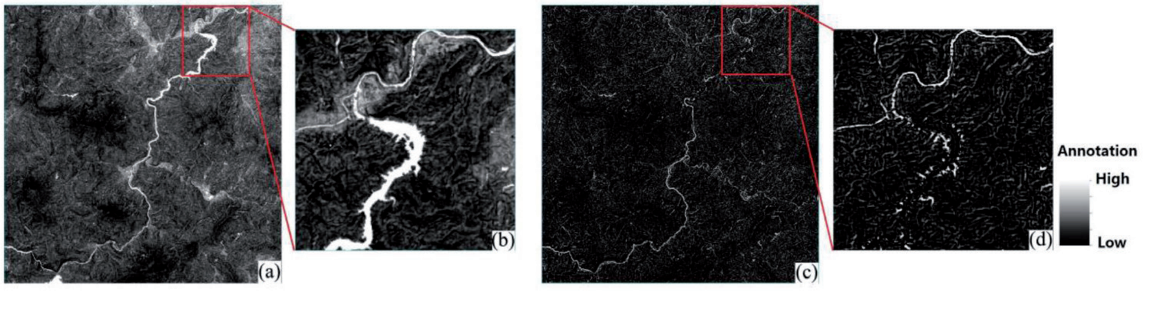

Figure 5.
Illustration of the linear enhancement and polygon compression of different land cover types in study area 3, where (a) and (c) are the MNDWI and the MNWI features, respectively, and (b) and (d) are the corresponding focused areas.

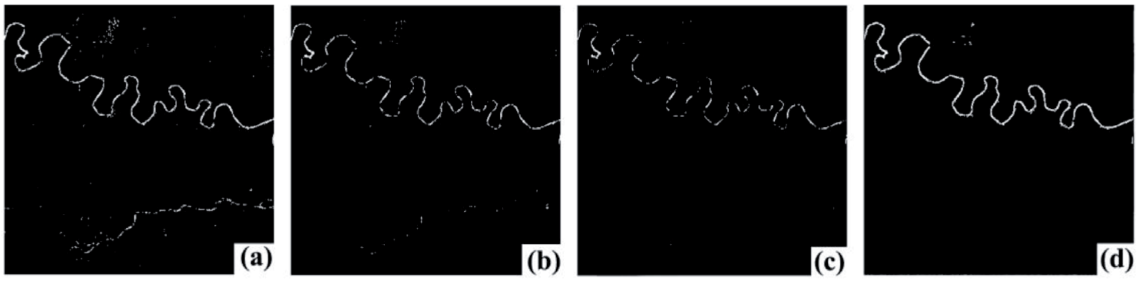

Figure 6.
Segmentation performed on the focused region of study area 1 using different thresholds, where (a), (b), and (c) are obtained by a threshold T equal to 20, 30, and 40, respectively, and (d) is the same image using a dual-threshold segmentation.

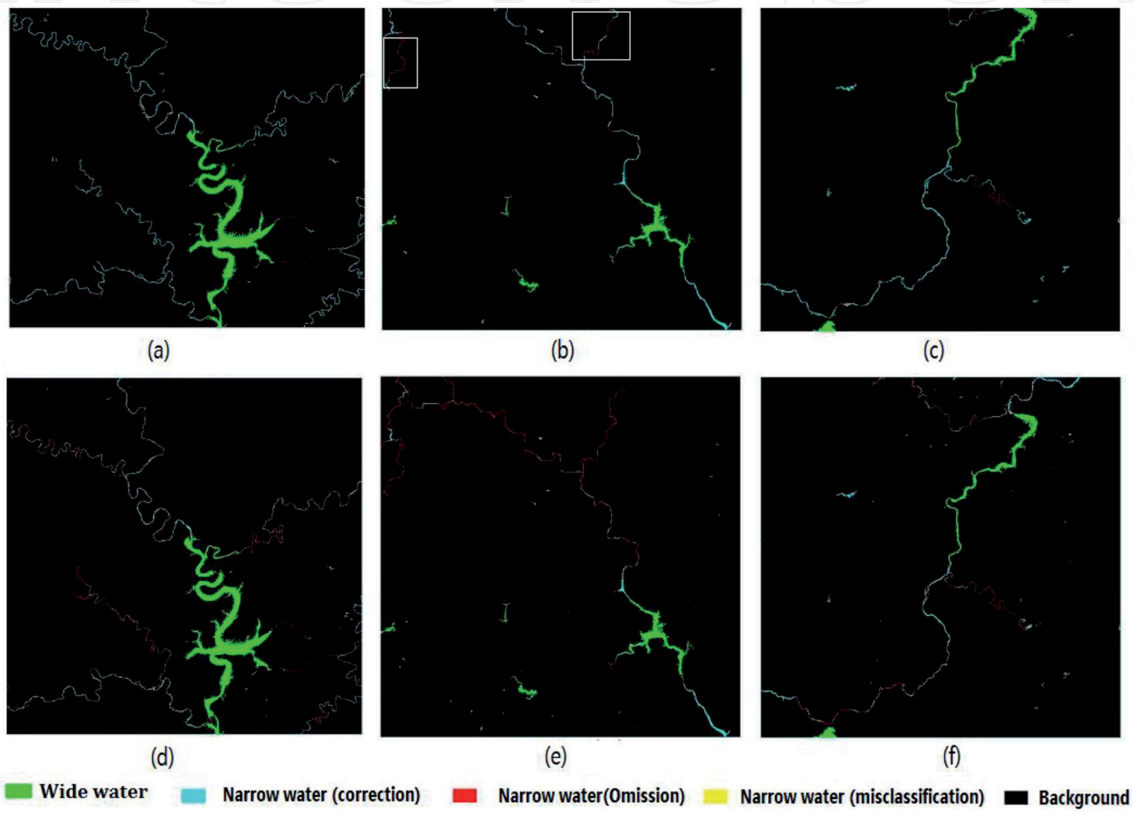

Figure 7.
Water extraction results from the three study areas, where the first and second lines are the results extracted by our method and the optimal threshold segmentation method, respectively.

clearly delineated in study area 1, and most narrow streams in study areas 2 and 3 are clearly extracted. However, a few narrow tributaries were misclassified by the MNDWI method, highlighted in red in **Figure 7**. A closer inspection of study area 2 shows that there are still two omissions which are highlighted with white rectangles, due to the width of two streams being too narrow (less than 10 m) to occupy a footprint, and the reflectance of these pixels are strongly mixed with other land cover types. Conversely, the results derived from the MNDWI image are less effective, as only small portions of the narrow rivers were extracted correctly. This is especially true for the narrow streams in the top region of the image, as most of them are ignored.

Another misclassification issue is the delineation of the sides of rivers, due to mixed pixel effects. Another experiment in the study area 3 was conducted to demonstrate this. These results are reported in **Figure 8**, where the water information that was corrected, omitted, and misclassified is shown in cyan, magenta, and red, respectively. It can be found that the boundary of the Youxi River can be accurately

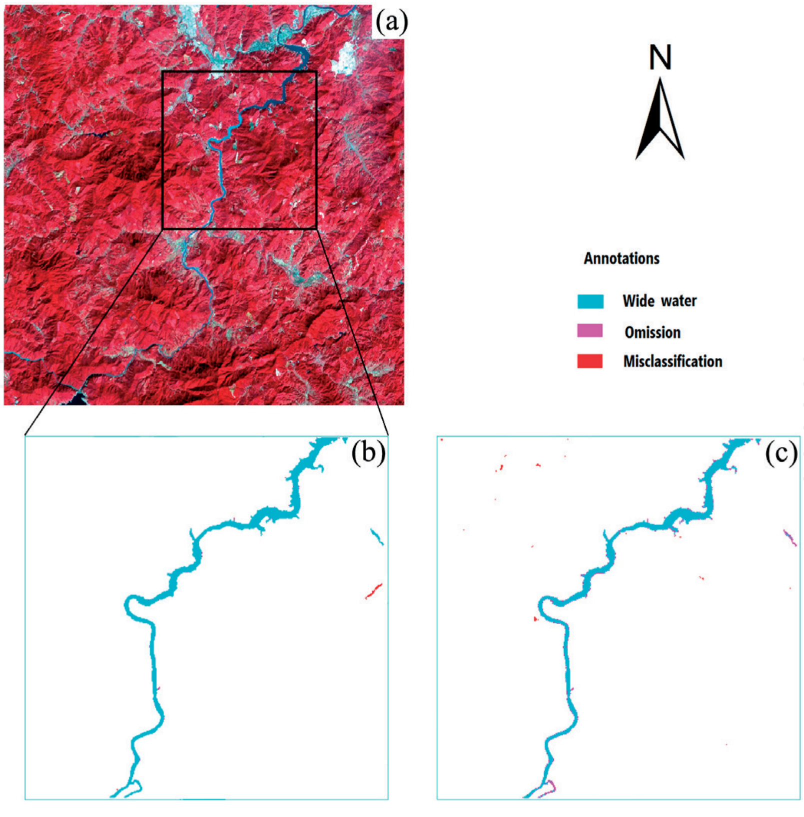

Figure 8.
The results of the river side misclassification experiment performed on study area 3. (a) the original image, (b) and (c) are the extracted water features in the focused area using out-proposed and the OT method, respectively.

extracted with the proposed method as shown in **Figure 8b**. However, using the MNDWI method with an optimal threshold, the omitted water pixels were along both sides of the river boundary (**Figure 8c**).

3.4 Quantitative evaluation

We now quantitatively evaluate our extracted results. Four measurements are used for comparison; the user and producer accuracy, the kappa coefficient, and the overall accuracy. Additionally, two recently developed methods for narrow water extraction, i.e., the method developed by Yang et al. [7] and the linear feature enhancement (LFE) developed by Jiang et al. [9], are also included for comparison. **Table 1** gives a pixel-by-pixel analysis of the classification accuracies for all datasets, with the best results highlighted in bold.

It can be seen in **Table 1** that the optimal threshold segmentation method was the least accurate, as it failed nearly completely in study area 2 with a 35% product accuracy and a kappa coefficient of 0.477. The method of Yang has some similar effects in narrow water extraction to our datasets, especially for mixed water features. The method of Jiang significantly improves the accuracy of narrow water extraction as compared to the optimal threshold segmentation method, as most of the narrow streams are well extracted in each of the study areas and had a comparable accuracy to our method. However, it should also be noted that this method is not an automatic method, since many parameters need to be tuned, which prevents it from being effectively used in larger areas. Overall, our method outperforms all others in terms of measurements except for producer accuracy in study area 3, where Yang's method achieves a relatively higher accuracy.

Methods		Optimal threshold	Yang	Jiang	Ours
Study area 1	Producer accuracy	53.8%	75.1%	92.1%	**92.3%**
	User accuracy	79.8%	85.3%	92.8%	**95.6%**
	Overall accuracy	67.3%	79.5%	91.3%	**93.6%**
	Kappa	0.631	0.748	0.907	**0.924**
Study area 2	Producer accuracy	35.2%	43.6%	82.8%	**83.9%**
	User accuracy	83.9%	57.6%	99.1%	**99.6%**
	Overall accuracy	55.4%	48.5%	89.2%	**90.7%**
	Kappa	0.477	0.453	0.872	**0.885**
	Producer accuracy	56.3%	55.5%	**87.1%**	86.9%
Study area 3	User accuracy	87.9%	73.8%	96.6%	**98.9%**
	Overall accuracy	71.2%	65.8%	90.3%	**91.6%**
	Kappa	0.696	0.627	0.881	**0.905**

Table 1.
Comparison of accuracies for different water extraction methods, with the best results given in bold text.

4. Extraction of inland water of Fujian province

The aforementioned experiments demonstrate that the MNWI is the most efficient algorithm for narrow water extraction, but it is still interest to address whether it is applicable to large-volume data in an actual scenario. Therefore, we apply our method to extract inland water features in Fujian province, China, which is a relatively large region that covers an area of about 121,000 km^2. Fujian is a mountainous province, located on the southeast coast of China and facing Taiwan across the Taiwan Strait. It has significant vegetation cover because of high mean precipitation and warm annual temperatures. Topographically, Fujian is a very mountainous region, having abundant water resources, rivers, lakes, and reservoirs. Many rivers run through these mountains, of which the most important is the Min River, as its drainage area covers over 50% of the province. The upstream Jin River, Futun River, and Shaowu River all converge into the Min River. The Jiulong River flows south of the Min River, reaching the sea at Xiamen city, and the Ting River runs across Fujian's southwestern border. It is thus an appropriate region to test our methods in a large area. To cover the entirety of Fujian province, 13 Landsat 8 OLI images were collected. Fujian is usually cloudy and rainy in spring and summer, so we collected all the images in winter to avoid cloud interference. The acquisition information is summarized in **Table 2**. Note that the quality of all acquired data is relatively good, with cloud cover less than 10%.

Path/row	118/041	118/042	119/041	119/042	119/043	120/040	120/041
Acquisition time	November 17	December 3	October 23	October 23	October 23	December 1	December 1
Path/row	120/042	120/043	120/044	121/041	121/042	121/043	
Acquisition time	December 1	December 1	December 1	October 5	October 5	October 5	

Table 2.
The information of collected Landsat 8 OLI images covering Fujian province in 2013.

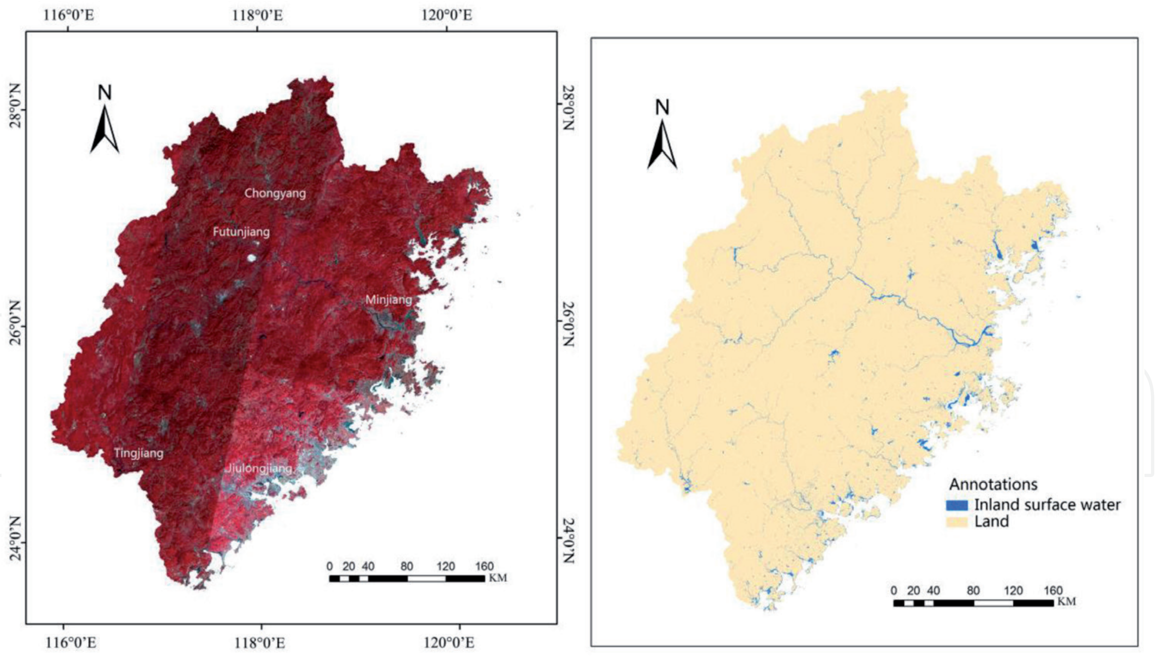

Figure 9.
The mosaic image and the final result of inland water bodies in Fujian province, China.

All the images were matched and stitched without altering their spectral color (**Figure 9**, left), and the final inland water information for the Fujian province (**Figure 9**, right) shows that 2,494,988 pixels were classified into inland surface water. It can be calculated that the total inland water area of Fujian province is about 2245.49 km^2 in the winter of 2013. Visually, our method can extract the most of perceptible water bodies with a high accuracy, where the main rivers, such as Min River, Jiurong River, Ting River, etc., are all correctly delineated with clear river boundaries. Moreover, most of the spatial shapes of small tributaries were continuous and so were the lakes and reservoirs. To evaluate the quantitative classification accuracy, 6800 samples of water and non-water features were randomly selected. The water samples included 3340 pixels, of which wide water to narrow water ratio was about 2:1, as the non-water samples were 3460 pixels, chosen from possibly confused land cover types such as forest, built-up areas, and rare soil. The producer accuracy, user accuracy, overall accuracy, and kappa coefficient calculated from these samples are 94.33%, 98.7%, 96.61%, and 0.932, respectively, indicating that the proposed method can achieve a high accuracy for water extraction in a large and complex area and it is an effective optional tool for practical water extraction.

5. Conclusions

Most water indices can perform well for the extraction of wide water features from remote sensing images, but they are normally ineffective in the extraction of narrow water features. This chapter has described a new method using a morphological top-hat transform to form a novel narrow water index, denoted as MNWI, which improves the extraction accuracy of narrow water from Landsat images. Experimental results demonstrated impressive performances of our method of the narrow water extraction. A case study in Fujian province suggests that it is an effective and practical tool for large area inland water.

Acknowledgements

Funding was provided by the Natural Science Foundation of China (Grant No. 41571330, 41830108).

Author details

Wu Bo[1]*, Zhang Jinmu[2] and Zhao Yindi[3]

1 School of Geography and Environment, Jiangxi Normal University, Nanchang, China

2 Key Laboratory of Poyang Lake Wetland and Watershed Research, Ministry of Education, Jiangxi Normal University, Nanchang, China

3 School of Environment and Spatial Informatics, China University of Mining and Technology, Xuzhou, China

*Address all correspondence to: mywubo@fzu.edu.cn

References

[1] Sun F, Sun W, Chen J, Gong P. Comparison and improvement of methods for identifying water bodies in remotely sensed imagery. International Journal of Remote Sensing. 2012;**33**:6854-6875

[2] Frazier PS, Page KJ. Water body detection and delineation with Landsat TM data. Photogrammetric Engineering and Remote Sensing. 2000;**66**:1461-1468

[3] Rokni K, Ahmad A, Solaimani K, Hazini S. A new approach for surface water change detection: Integration of pixel level image fusion and image classification techniques. International Journal of Applied Earth Observation and Geoinformation. 2015;**34**:226-234

[4] McFeeters S. The use of the normalized difference water index (NDWI) in the delineation of open water features. International Journal of Remote Sensing. 1996;**17**:1425-1432

[5] Xu H. Modification of normalised difference water index (NDWI) to enhance open water features in remotely sensed imagery. International Journal of Remote Sensing. 2006;**27**:3025-3033

[6] Carleer AP, Wolff E. Urban land cover multi-level region-based classification of VHR data by selecting relevant features. International Journal of Remote Sensing. 2006;**27**(6):1035-1051

[7] Yang S, Xue S, Liu T. Method for automatically extracting fine water body by using TM image. Journal of Surveying and Mapping (in Chinese with English Abstract). 2010;**39**(6):611-617

[8] Li Y, Ding J, Yan R. Study on extraction method of small water bodies in mountainous area based on GF-1 remote sensing images. Resource Science (in Chinese with English Abstract). 2015;**37**(2):408-416

[9] Jiang H, Feng M, Zhu Y. An automated method for extracting rivers and lakes from Landsat imagery. Remote Sensing. 2014;**6**(6):5067-5089

[10] Beneditsson JA, Pesaresi M, Arnason K. Classification and feature extraction for remote sensing images from urban area based on morphological transformations. IEEE Transaction on Geosciences and Remote Sensing. 2003;**41**(9):1940-1949

[11] Huang X, Zhang L. A multidirectional and multi-scale morphological index for automatic building extraction from multispectral GeoEye-1 imagery. Photogrammetric Engineering & Remote Sensing. 2011;**77**(7):721-732

[12] Wu B, Fang C, Yu L, Huang X, Zhang Q. A fully automatic method to extract rare earth mining area from Landsat image. Photogrammetric Engineering and Remote Sensing. 2016;**82**(9):55-64

[13] Huang X, Zhang L, Wang L. Evaluation of morphological texture features for mangrove forest mapping and species discrimination using multispectral IKONOS imagery. IEEE Geoscience and Remote Sensing Letters. 2009;**6**(3):393-397

[14] Ji L, Zhang L, Wylie B. Analysis of dynamic thresholds for the normalized difference water index. Photogrammetric Engineering and Remote Sensing. 2009;**75**(11):1307-1317

[15] Otsu N. A threshold selection method from gray-level histograms. IEEE Transactions on Systems, Man and Cybernetics. 1979;**9**(1):62-66

[16] Zha Y, Gao Y, Ni S. Use of normalized difference built-up index in automatically mapping urban areas from TM imagery. International Journal of Remote Sensing. 2003;**24**(3):583-594